Nuclear Materials and Energy 000 (2016) 1–4

Contents lists available at ScienceDirect

Nuclear Materials and Energy

journal homepage: www.elsevier.com/locate/nme

Post mortem analysis of a tungsten coated tile from the outer divertor strike point region of ASDEX upgrade

E. Fortuna-Zalesna[a,*], M. Andrzejczuk[a], L. Ciupinski[a], K. Rozniatowski[a], K. Sugiyama[b], M. Mayer[b], K.J. Kurzydlowski[a], ASDEX Upgrade. Team

[a] Warsaw University of Technology, 02-507 Warsaw, Poland
[b] Max-Planck-Institut für Plasmaphysik, D-85748 Garching, Germany

ARTICLE INFO

Article history:
Available online xxx

Keywords:
Erosion
Re-deposition
Divertor
Electron microscopy
ASDEX-Upgrade
PFCs lifetime

ABSTRACT

In the present study, the structure and the composition of co-deposited layers developed at the outer divertor strike point tile 1 in ASDEX Upgrade during three campaigns from 2009 to 2013 were examined. The samples were cut from representative locations which differed in received flux: private flux, strike point, the highest plasma fluence and "moderate" flux regions. High resolution scanning (SEM) and transmission electron microscopy (HRSTEM) combined with energy-dispersive X-ray spectroscopy (EDS) and optical profilometry have been used to identify deposits composition and morphology as well as to assess coating degradation. The aim of the post-mortem analyses was the evaluation of materials mixing and evidence of plasma-induced damage.

Our results confirm that the outer divertor of AUG is generally a net erosion region for tungsten, however, the strong deposition of eroded tungsten takes place close to the outer strike point (private flux region). The observations on cross-sections of the tungsten coatings revealed micro-cracks around the strike point region. These cracks are caused by thermal stresses due to periodic heating and cooling of the layer during ELMs.

1. Introduction

Tungsten (W) is a candidate material for the ITER divertor [1,2]. A detailed understanding of the in-service performance of W plasma-facing components (PFCs) is essential for assessing their degradation by plasma interactions and formation of mixed materials. In the current and the past fusion experiments tungsten has been used both as a bulk material and as coatings deposited (by evaporation and plasma-spraying) on carbon substrates (TEXTOR, ASDEX Upgrade, JET and JT-60U) [3–5].

In the present work the performance of the tungsten coating in the ASDEX Upgrade divertor has been investigated in the context of: (a) the erosion and deposition pattern at the outer divertor strike point region and (b) damage of the material caused by the power loads from a fusion plasma.

The outer strike point (OSP) region of ASDEX Upgrade has been chosen for the post mortem analysis since in this region both erosion and re-deposition are known to play the largest role [4,6–8]. This work is a continuation of our studies concerning examination of the structure and the composition of co-deposited layers, which developed at the OSP tile 1 after one experimental campaign in 2009 [6].

2. Experimental

The investigations were carried out at four samples from the outer divertor tile no 1 of ASDEX Upgrade, exposed to the conditions of three campaigns in the period 2009–2013. These samples were cut from representative locations and differed in the received flux, as described in Table 1 and in Fig. 1. The total fluence onto the outer divertor was in the range of 10^{26} m^{-2}. The machine operated with relatively low heating power input in 2009, mostly below 10MW. Higher heating power was exercised in the later campaigns. For details concerning particular experimental campaigns see [7–9]. The tile was coated with a tungsten layer using the combined magnetron sputtering and ion implantation method (CMSII) [10]. The initial thickness was approximately 12 µm. A 2–3 µm thick Mo interlayer was deposited between the tungsten layer and

* Corresponding author.
E-mail address: efortuna@o2.pl (E. Fortuna-Zalesna).

http://dx.doi.org/10.1016/j.nme.2016.10.011

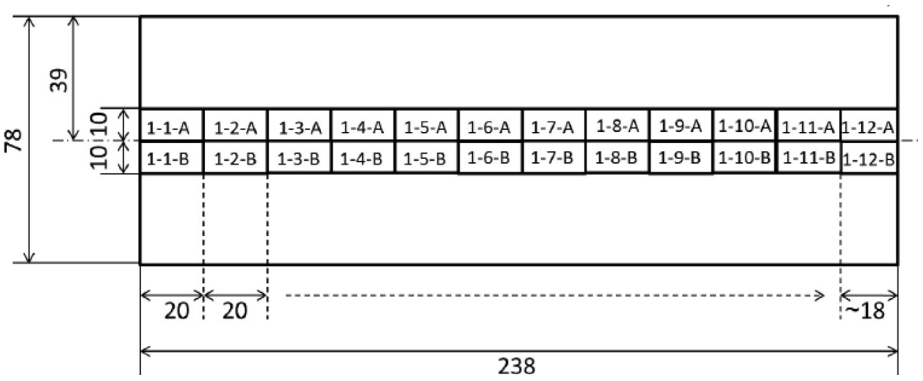

Fig. 1. Drawing of Tile 1 explaining sampling locations. All dimensions in mm.

Table 1
Samples description.

Name	Description
1-1A	private flux region, limited plasma contact, thick co-deposition
1-3A	strike point region, exposed to high heat load
1-4A	the highest plasma fluence region
1-10A	"moderate" region

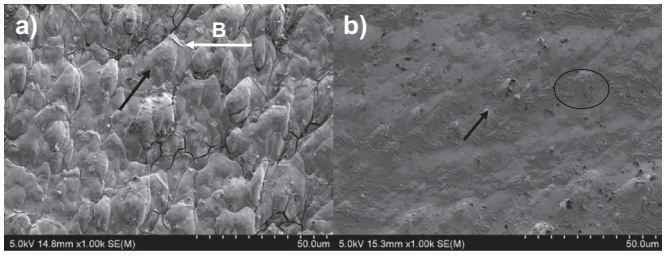

Fig. 2. SEM images of the coating morphology of sample 1-1A, (a), and 1-3A, (b). Black arrows indicate the direction of the erosion, whereas the white arrow in (a) indicates the direction of the lines of the toroidal magnetic field. Deposit is encircled in the oval – see the stratified, wavy area, where re-deposited material was sequentially accumulated (b).

the graphite substrate in order to improve the adhesion of the layer.

The surface morphology investigations were performed with a Hitachi SU-70 FE-SEM scanning electron microscope combined with energy-dispersive X-ray spectroscopy (EDS) using Thermo Scientific Ultra Dry and YAG BSE (backscattered electrons) detectors. The structure of the surface layers was determined by cutting samples with a focused ion beam (FIB/SEM Hitachi NB5000) and examining with scanning transmission electron microscopy (STEM, Aberration Corrected Dedicated STEM Hitachi HD-2700). The surface morphology was quantified with the use of optical profilometer VeecoWyko NT 9300.

3. Results

SEM examinations revealed that the surface of all examined samples was modified due to exposure to the conditions of the 2009–2013 campaigns as evidenced by the images in Fig. 2. The investigated samples have distinctly smoother surfaces in comparison to their initial morphology, which has been described in [6]. The surface shows a specific erosion/deposition patterns in the form of: (i) elongated remains of the initial grain structure, which are at an angle of approximately 45° to the lines of the toroidal magnetic field and (ii) deposits in the shadowed areas.

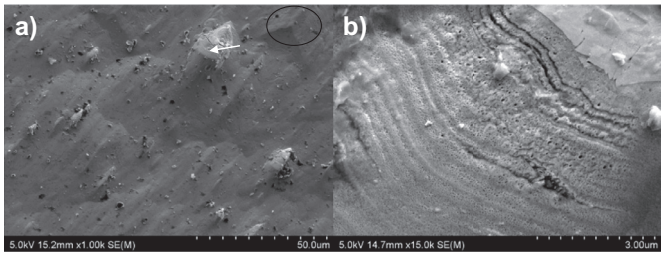

Fig. 3. SEM images of the coating and deposit morphology: a) sample 1-4A, b) sample 1-10A. Deposit is encircled in the oval.

The highest roughness has been measure for the sample 1-1A shown in Fig. 2a. The surface is covered by a thick, cracked, stratified deposit of good adhesion to the coating. Small fragments of deposit are chipped off, very likely contributing to the dust production.

The surface morphology of the three other samples is different. They exhibit a more pronounced surface smoothening, as evidenced by the SEM images in Figs. 2b and 3a. Their surface is also covered by deposit, however, of a different character, with a tungsten-based, sponge like structure shown in Fig. 3b. Solid layers, rich in boron were also found. The thickness of the deposit is inhomogeneous and higher in the shadowed areas, as indicated in Figs. 2b and 3a. Particles rich in boron were also found and elongated artefacts as observed already before by M. Balden [11] – see Fig. 3a.

The morphology of the samples surfaces as described above agrees with the results of the measurements of surface roughness. Sample 1-1A is characterized by the highest value Ra = 1500 nm. The surface roughness of the samples 1-3A and 1-4A is at similar level Ra = 820 and 735 nm, respectively. The surface of sample 1-10A is the smoothest with Ra = 490 nm.

It should be noted that the surfaces of samples 1-3A and 1-4A, which were from the strike point and the highest plasma fluence region respectively, revealed a network of cracks shown in Fig. 4. The examinations of coating cross-sections revealed that these cracks go through the entire CMSII-W and Mo (inter)-layers down to the graphite substrate. It is worth noting that cracks and other defects have also been revealed underneath the surface of the tungsten layers (see Fig 5). Thus, it can be concluded that the cracks observed are very likely to initiate at the graphite/molybdenum interface.

The observations on cross-sections of the coatings, prepared by FIB – see Fig. 5 - showed the same thickness of the tungsten and molybdenum layers, ~12.5 and ~2.5 µm, respectively. The thickest deposit, up to 6.5 µm, was found in sample 1-1A. The deposit on sample 1-10A was the thinnest and not covering the entire surface.

Please cite this article as: E. Fortuna-Zalesna et al., Post mortem analysis of a tungsten coated tile from the outer divertor strike point region of ASDEX upgrade, Nuclear Materials and Energy (2016), http://dx.doi.org/10.1016/j.nme.2016.10.011

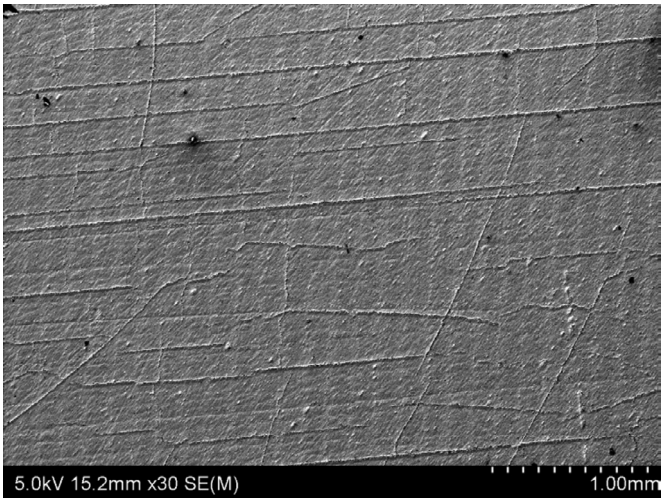

Fig. 4. SEM image of cracks on the surface of 1-4A sample.

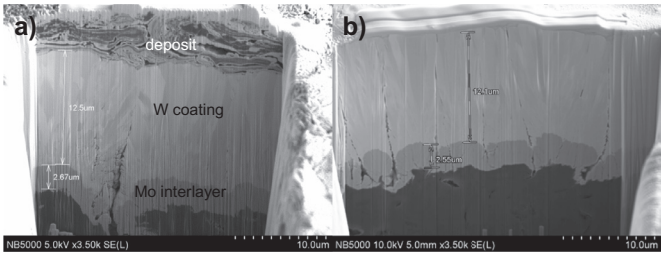

Fig. 5. SEM images of the coating cross-sections: a) sample 1-1A and b) sample 1-10A.

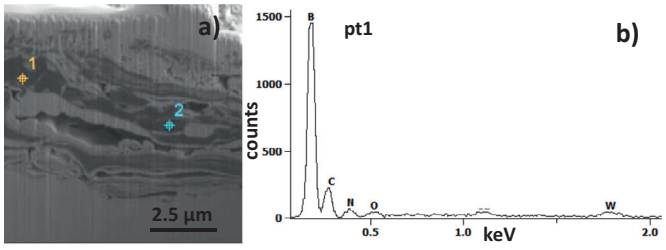

Fig. 6. SEM image of the deposit present at the sample 1-1A cross-section (a) and the corresponding EDS spectrum (b).

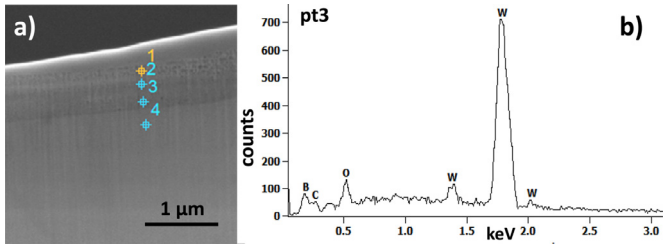

Fig. 7. SEM image of the deposit present at the sample 1-3A cross-section (a) and the corresponding EDS spectrum (b).

In sample 1-1A crystals rich in boron and pores up to several microns long were found.

The EDS measurements showed that the components of the deposit are tungsten, oxygen and boron – Figs. 6 and 7. Nitrogen, carbon and iron were also detected. The EDS measurements performed both at the FIB cross-sections and thin foils indicated the higher boron content in the deposit cut from the private flux region (Figs. 6, 7, 9).

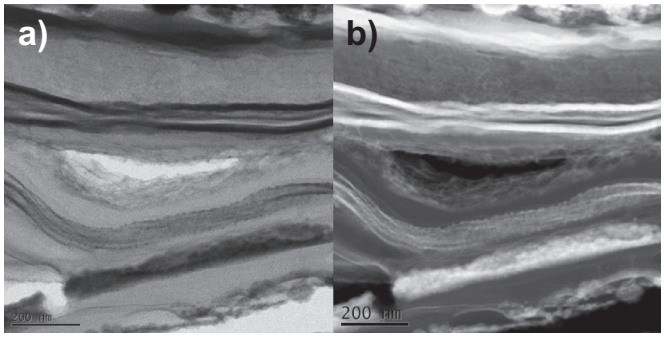

Fig. 8. STEM images of the deposit on sample 1-1A: a) bright field (BF) mode and b) HAADF mode.

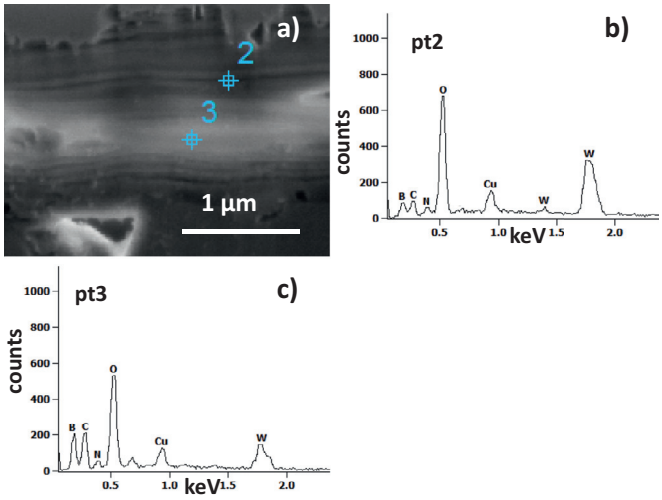

Fig. 9. SEM image of the deposit present at the sample 1-1A cross-section (a) and the corresponding EDS spectra (b-c).

3.1. TEM examinations

The structure of the deposit was investigated by STEM observations of thin lamellas cut by FIB. In the case of sample 1-1A in the lamella cut from the "flat" region, a stratified structure of deposited material has been revealed with sub-layers having thicknesses up to 200 nm – see Fig. 8. Observations using a high angle annular dark field (HAADF) mode, also called Z-contrast, proved differences in their chemical composition. The bright stripes visible in Fig. 8b are enriched in heavy elements i.e. tungsten, whereas the dark ones are rich in light elements - boron and carbon. The EDS spectra from the deposit region are presented in Fig. 9. The signal from copper comes from the copper grid the FIB lamella is mounted on.

The deposit on the samples designated as 1-3A, 1-4A and 1-10A is similar and reveals re-deposited tungsten in the form of a three dimensional sponge-like structure illustrated in Fig. 10. The structure is inhomogeneous with "sponge cells" sizes varying from a few to several tens of nm. It contains re-deposited tungsten together with boron and carbon, Fig. 7. Diffraction patterns from the deposit area proved the presence of both amorphous and crystalline matter, as shown in Fig. 11.

4. Discussion

The outer strike point divertor tile 1 coated with CMSII tungsten and exposed in the machine for three campaigns from 2009 to 2013 was analysed to provide data on materials mixing and

Please cite this article as: E. Fortuna-Zalesna et al., Post mortem analysis of a tungsten coated tile from the outer divertor strike point region of ASDEX upgrade, Nuclear Materials and Energy (2016), http://dx.doi.org/10.1016/j.nme.2016.10.011

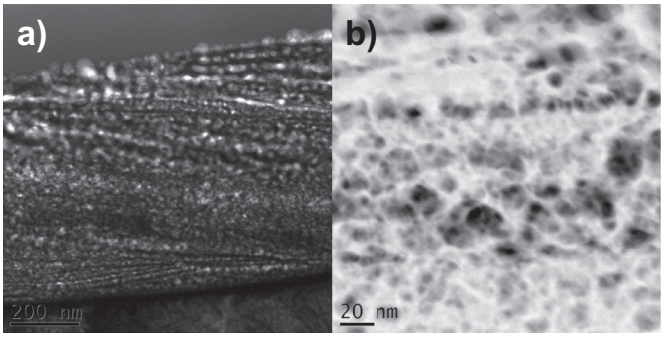

Fig. 10. STEM images of deposit present at sample 1-3A: a) BF mode, b) HAADF mode.

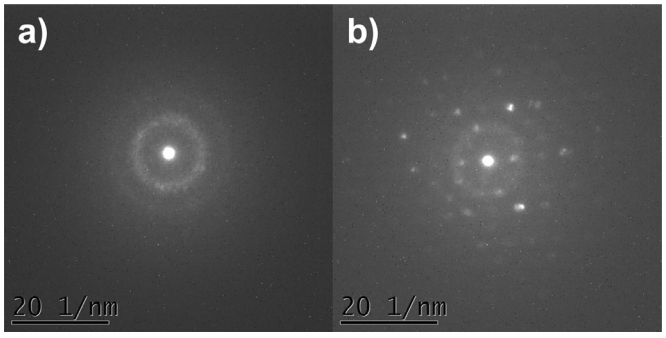

Fig. 11. Diffraction patterns from deposit present in Fig. 9a.

plasma-induced damage of the tungsten coating. In this context it should be noted that the outer surface of all samples changed its morphology. The changes in the morphology were induced by two processes: (a) erosion and (b) re-deposition.

As a result of erosion the samples have distinctly smoother surfaces in comparison to the initial morphology [6]. The analysis of A. Hakola [8] concerning the long-term erosion patterns of tungsten coatings in the OSP region in AUG showed that rough parts of coatings eroded and most of the eroded material had been re-deposited together with boron, deuterium and carbon on the shadowed areas of the most protruding surface features. On the smoother surfaces the deposited layers were much thinner, which is in agreement with our observations. Also, it should be noted that the erosion has a clear directional character, with elongated features (residue of the initial tungsten grain structure) at an angle of ~45° with respect to the lines of the magnetic field. This characteristic orientation of elongated features was reported earlier by M. Balden [11], who studied the surface of polished tungsten specimens after exposure to the outer divertor plasma close to the strike point in the 2011 campaign. Porous, layered deposits formed around dust particles stacked at the surface, with an elongation at an angle of approximately 45° to the B field lines.

In discussion of the results obtained it should be noted that re-deposited material was found on all of the examined samples, however, appearing with varying thickness. Relatively thick deposited layers were formed in shadowed areas, with the thickest, up to 6.5 µm on the sample 1-1A collected from the private flux region. Examinations of the deposit structure revealed crystals rich in boron and sub-layers up to 200 nm thickness of differed chemical composition on this sample. Such a structure is typical for layers formed in the inner divertor baffle region. The crystals rich in boron found in AUG dust particles were examined in [12] and identified as boron carbide. The mechanisms responsible for the strong net deposition in the private flux region are described elsewhere [13].

The deposit on three other samples (strike point region, the highest plasma fluence and moderate regions) was thinner and had a sponge-like structure. The porous tungsten structure was observed first by M. Rasinski [6] at the outer strike point divertor tile exposed in AUG after one experimental campaign in 2009. The examined deposits were distinctly thinner in comparison to the layers observed in the present studies, with the thickness varying from 200 up to 1500 nm, depending on the sample location.

The composition of deposited material, namely tungsten with boron, nitrogen, carbon and oxygen, is typical for AUG [6,11,14]. Nitrogen comes from impurity seeding experiments started in 2009 [10], boron from regular boronization of the vessel [15] and oxygen from air uptake. Additionally, in our work locally small amounts of iron were detected. Iron is a component of stainless steel used in AUG as structural material (SS301) for example in the main chamber.

Based on our microscopy studies we cannot access quantitatively how much of material was eroded from the examined locations because we do not know precisely the initial thickness of the coating. The net erosion rates of the outer strike point region of AUG were, however, examined by experiments with the use of marker tiles. The results concerning the 2009 and 2010-11 campaigns are given in [7,8] respectively. It could be, however, observed that the CMSII-W layer preserved its thickness of approximately 12 µm after three campaigns of AUG operation at high flux/heat-load region, i.e. the net erosion was comparatively small. The observations on cross-sections revealed, however, micro-cracks around the strike point region. These cracks are induced by thermal stresses due to periodic heating and cooling of the layer during ELMs. The observed cracks extend through the entire CMSII-W layer and the Mo interlayer down to the graphite substrate.

Our results confirm that the outer divertor of AUG is generally a net erosion region for tungsten [4,7,8]. Strong deposition of eroded tungsten, however, takes place close to the outer strike point.

Acknowledgment

This work has been carried out within the framework of the EUROfusion Consortium and has received funding from the European Union's Horizon 2020 research and innovation programme under grant agreement number 633053. The views and opinions expressed herein do not necessarily reflect those of the European Commission.

References

[1] T Hirai, et al., Fusion Eng. Des. 88 (2013) 1798–1801.
[2] R Villari, et al., Fusion Eng. Des. 88 (2013) 2006–2010.
[3] E. Fortuna, et al., Phys. Scr. T128 (2007) 162–165.
[4] M. Mayer, et al., Phys. Scr. T138 (2009) 014039.
[5] R. Neu, et al., J. Nucl. Mater. 438 (2013) S34–S41.
[6] M Rasinski, et al., Fusion Eng. Des. 86 (2011) 1753–1756.
[7] A Hakola, et al., J. Nucl. Mater. 463 (2015) 162–165.
[8] A. Hakola, et al., Phys. Scr. T159 (2014) 014027.
[9] K. Sugiyama, et al., Phys. Scr. T159 (2014) 014043.
[10] C. Ruset, E. Grigore, H. Maier, et al., Phys. Scr. T128 (2007) 171.
[11] M. Balden, J. Nucl. Mater. 438 (2013) S220.
[12] E Fortuna-Zalesna, et al., Phys. Scr. T 159 (2014) 014066.
[13] A. Hakola, et al., Phys. Scr. T159 (2016) 014026.
[14] A. Kallenbach, et al., J. Nucl. Mater. 415 (2011) S19–S26.
[15] A Kallenbach, et al., Nucl. Fusion 49 (2009) 045007.

Please cite this article as: E. Fortuna-Zalesna et al., Post mortem analysis of a tungsten coated tile from the outer divertor strike point region of ASDEX upgrade, Nuclear Materials and Energy (2016), http://dx.doi.org/10.1016/j.nme.2016.10.011